Reassessing the Strategies for Trapping Catalytic Intermediates during Nitrate Reductase Turnover

Vincent Fourmond,[†] Monique Sabaty,[‡] Pascal Arnoux,[‡] Patrick Bertrand,[†] David Pignol,[‡] and Christophe Léger*,[†]

Unité de Bioénergétique et Ingénierie des Protéines, Institut de Microbiologie de la Méditerranée, Centre National de la Recherche Scientifique, UPR 9036, 31 Chemin Joseph Aiguier, 13402 Marseille Cedex 20, France, Laboratoire de Bioénergétique Cellulaire, Commissariat à l'Energie Atomique, DSV, IBEB, F-13108 Saint-Paul-lez-Durance, France, Centre National de la Recherche Scientifique, UMR 6191, Biologie Végétale et Microbiologie Environnementale, 13108 Saint-Paul-lez-Durance, France, and Aix-Marseille Université, 3 Place Victor Hugo, 13333 Marseille Cedex 3, France

Received: December 2, 2009; Revised Manuscript Received: January 18, 2010

We examined the kinetics of nitrate reduction by periplasmic nitrate reductase (Nap) by using protein film voltammetry and solution assays. We demonstrate that, under turnover conditions, the enzyme exists as a mixture of active and inactive forms which interconvert on a time scale that is much slower than turnover. The dead-end species accumulates under mildly reducing conditions and at high nitrate concentration, resulting in substrate inhibition and in an uncommon hysteresis in the voltammetric signature. Solution assays with two electron donors having different reduction potentials fully support the electrochemical results. This illustrates the consequences of the high flexibility of the active site molybdenum coordination sphere and questions the conclusions from earlier studies in which attempts were made to trap catalytic intermediates of Nap in experiments carried out under turnover conditions at very high substrate concentration.

A common strategy for studying the mechanism of metalloenzymes is to generate and trap during turnover catalytic intermediates in high concentration and to use various spectroscopic techniques to characterize the structure of their active site. When a signal is obtained during turnover, evidence of it being a state along the reaction pathway, rather than a dead-end, may be supported by the observations that (i) the product is actually being formed under the conditions used to trap the putative intermediate; (ii) after initiation of the reaction, the intermediate appears on a time scale that is comparable to turnover; and (iii) its steady-state concentration correlates with the turnover rate when the substrate concentration is varied (see, e.g., the case of nitrogenase in ref 1 and ref 2 for review). These control experiments cannot always be carried out, and it may occur that certain spectral signatures once considered as arising from catalytic intermediates will eventually turn out to be inactive states or artifacts. Here we demonstrate that periplasmic nitrate reductase (Nap), a mononuclear molybdenum enzyme of the dimethyl sulfoxide (DMSO) reductase family, exemplifies the worst-case scenario: in addition to a previous finding that its "as prepared" form requires irreversible activation, we demonstrate here that the enzyme reversibly interconverts between active and inactive states, the latter actually accumulating under conditions that were always presumed to favor the formation of catalytic intermediates. These (in)activation processes attest to the existence of various inactive states that are formed under distinct conditions. Protein film voltammetry proves invaluable for detecting these states and determining the conditions under which they are produced.

Rhodobacter sphaeroides (*R. spheroides*) periplasmic nitrate reductase (NapAB)[3] catalyzes the reduction of nitrate to nitrite, using electrons from the quinone pool. The active site of NapAB is the mononuclear molybdenum bis(molybdopterin) cofactor which characterizes the enzymes of the so-called DMSO reductase family.[4–7] These enzymes specifically catalyze distinct oxo-transfer reactions, such as the reduction of nitrate or DMSO or the oxidation of arsenite, but little is known about which structural details determine this substrate specificity.

The catalytic mechanism of Nap has been studied using a variety of biophysical techniques, including crystallography[3,8] and electron paramagnetic resonance (EPR) spectroscopy; the latter is used in particular to detect and characterize the coordination sphere of the Mo in the +5 state. According to the most commonly accepted mechanism, nitrate reacts with the Mo(IV) ion, producing Mo(VI) which is rereduced to Mo(IV) in two one-electron steps, via a Mo(V) species.[9] Although various alternative mechanisms have recently been proposed and discussed,[8,10,11,37] the involvement of a Mo(V) intermediate in the catalytic cycle was never questioned. Distinct Mo(V) EPR signals have been detected under various conditions (see refs 7, 12, and 13 for review), but which or whether any of these signals arises from a catalytic intermediate is still uncertain. On the contrary, we have shown recently that the main EPR signature of the active site in the "as-purified" periplasmic nitrate reductase of *R. sphaeroides*, the so-called "Mo(V) high-*g* signal," is actually that of a dead-end species which irreversibly becomes catalytically competent only after full reduction.[13]

Such irreversible reductive activation also occurs in another enzyme of this family: the DMS-*oxidation* activity of periplasmic DMSO reductase increases significantly after the enzyme

* To whom correspondence should be addressed. Tel.: +33 4 91 16 45 29. Fax: +33 4 91 16 40 97. E-mail: christophe.leger@ifr88.cnrs-mrs.fr.
[†] Centre National de la Recherche Scientifique, UPR 9036, and Aix-Marseille Université.
[‡] Commissariat à l'Energie Atomique, Centre National de la Recherche Scientifique, UMR 6191, and Aix-Marseille Université.

10.1021/jp911443y
Published on Web 02/17/2010

has been fully *reduced*.[14] It was long undetected in NapAB because measuring the nitrate reductase activity requires that the sample be reduced, and reduction irreversibly activates the enzyme. Therefore, detecting it requires that the activity be sampled faster than the activation proceeds; this cannot be achieved in traditional assays with soluble electron donors, but protein film voltammetry (PFV),[15] where the enzyme is adsorbed onto an electrode surface and the activity is measured as a current, provides ideal temporal resolution and potential control.

In this paper, we use PFV to demonstrate that, after the initial, *irreversible* reductive activation whose study is reported in ref 13, the active form of NapAB slowly and *reversibly* converts into an inactive form when the potential and/or the nitrate concentration is increased. Solution assays confirm that the enzyme is inactivated by a large excess of nitrate provided the electrons come from a high potential electron donor. This reversible inactivation process is unprecedented in molybdenum enzymes.

Our findings will impact the methods and strategies for studying the catalytic mechanism of nitrate reductase. Indeed, that the enzyme is slowly inactivated by a large concentration of substrate questions the interpretation of earlier studies according to which species trapped under turnover conditions at very high substrate concentration are intermediates in the catalytic cycle.

Results

Periplasmic nitrate reductases from *Paracoccus pantotrophus* (*P. pantotrophus*)[16] and *R. sphaeroides* (our work) make very stable enzyme films when adsorbed onto a pyrolytic graphite edge (PGE) electrode. Electron transfer from the electrode to the enzyme is direct and fast, and the activity is detected as a negative current whose magnitude is proportional to the turnover rate. If the electrode is rotated at a high rate, the limitation from mass transport is released and the signal discloses the intrinsic properties of the enzyme. Since the electroactive coverage is unknown, the actual value of the turnover rate cannot be measured (only a lower limit can be estimated; cf. note 34 in ref 13), but even a small change in activity is accurately and instantly detected as a change in current. This is very useful when the enzyme activates or inactivates over time, as illustrated below.

Voltammetry. The cyclic voltammogram shown in Figure 1A (plain line) was recorded with *R. sphaeroides* NapAB adsorbed onto a rotating disk PGE electrode, in a solution at pH 6 containing 10 μM nitrate, after the enzyme had been reductively activated as described previously.[13] The forward and backward sweeps are identical and only offset by the capacitive current (resulting from electrode "charging"). The voltammogram is therefore a simple readout of steady-state activity against potential. It displays an extremum at about −100 mV vs SHE (Figure 1A). This feature has been observed with many enzymes of the DMSO reductase family (see refs 15 and 18 for review) and also with a mononuclear molybdenum enzyme of the sulfite oxidase family.[19] It is believed to relate to (and inform on) the chemistry that occurs at the active site during the catalytic cycle[15,20–22] (see, however, ref 16). The relation between the shape of the steady-state electrochemical signal and the results of solution assays is discussed in ref 22.

The catalytic voltammograms recorded under slightly acidic conditions and greater nitrate concentrations are different. At $[NO_3^-] \geq 4$ mM at pH 6 or ≥ 1 mM at pH 5.5 for example, they exhibit a pronounced hysteresis above −200 mV, as exemplified in Figure 1B: the current measured during the forward scan (toward negative potentials) is smaller than that during the return scan. We rule out that this is caused by a reorientation of the enzyme on the electrode, because we never observed any hysteresis in experiments carried out with several mutants of the enzyme where an amino acid that is buried deep in the protein has been exchanged (see, e.g., in Figure 1C the voltammogram of the R392A variant[17]). The perfect agreement between results of PFV experiments and solution assays (see, as follows, the discussion of Figure 4) will also support the conclusion that the hysteresis in Figure 1B reveals an intrinsic property of the enzyme.

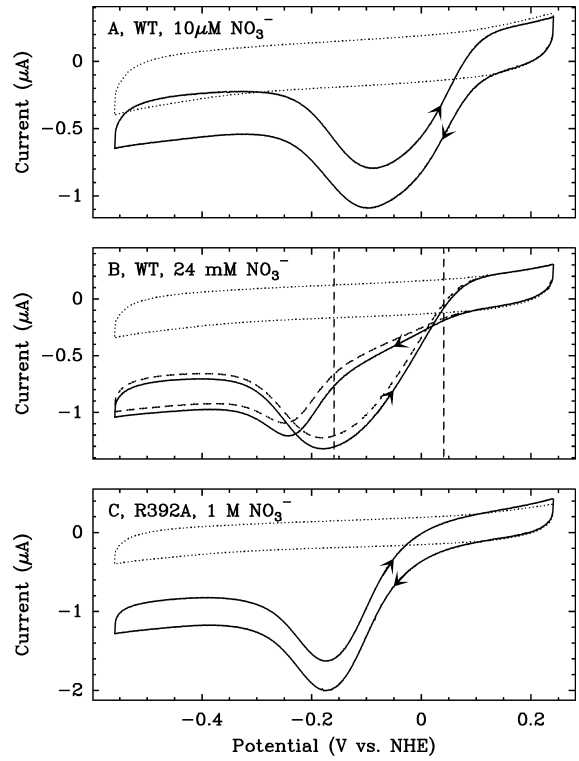

Figure 1. Cyclic voltammograms of *R. sphaeroides* NapAB adsorbed on a rotating-disk pyrolytic graphite "edge" electrode, at pH 6, 25 °C, a scan rate of 20 mV/s, and an electrode rotation rate of 5 krpm. Panel A shows the usual steady-state catalytic response obtained with the wild-type (WT) enzyme, in the presence of 10 μM nitrate (plain line); the dotted line is a blank recorded with no adsorbed enzyme. The arrows indicate the direction of the sweep. Panel B: with the WT enzyme, a large hysteresis is visible at high nitrate concentration (24 mM). The dashed line is the scan following immediately the solid line; the only difference is a decrease in the amplitude of the signal due to film loss. The vertical dashed lines on panel B mark the range of electrode potentials used in the chronoamperometric experiments of Figure 2. Panel C shows a voltammogram recorded with the R392A NapAB mutant[17] at 1 M nitrate.

In the experiment in Figure 1B, the increase in current magnitude occurs during the scan across several hundreds of millivolts at a scan rate of 20 mV/s, corresponding to a rate constant of about 0.1 s^{-1}. This is much slower than the turnover rate, which is of the order of hundreds per second.[13] Thus, the hysteresis is not caused by the departure from the steady state of the catalytic cycle (very fast scan rates can outrun catalysis, but this requires that the voltammetric time scale approaches the characteristic time of turnover[23]). Rather, the hysteresis reveals a slow interconversion between active and inactive forms of the enzyme; by "inactive" here, we mean that this form is not encountered during turnover, and stands apart from the normal reaction pathway.

This activation process is fully reversible, since any two successive voltammograms are identical except for a small

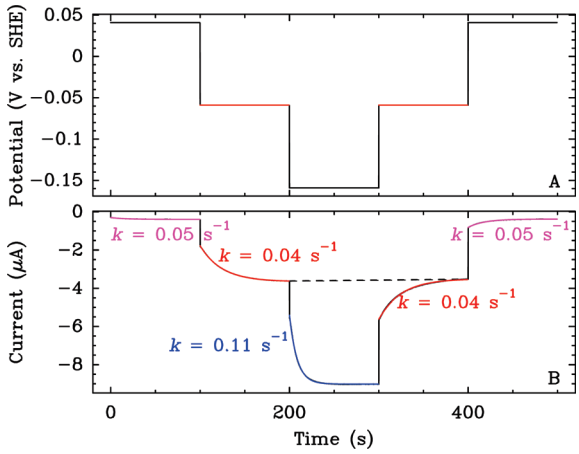

Figure 2. Relaxation toward a new steady state after stepping the electrode potential. Panel A shows the potential that was applied. Panel B shows the resulting current. The rate constants k determined by fitting each transient to an exponential are indicated for each step. Note that at −60 mV, for example, the rate constant of the relaxations (red lines) is independent of whether the enzyme is activating (t = 100−200 s) or inactivating (300−400 s), and the asymptotic value of the current at t = 200 and 400 s is also the same (this is marked by the horizontal dashed line). The relaxation plotted in purple corresponds to the same conditions as those of the purple transient in Figure 3. The data were corrected for film loss as described previously;[24] the raw data are shown on Supporting Information Figure S2. Conditions: pH 6; 25 °C; 7.5 mM nitrate; electrode rotation rate, 5 krpm.

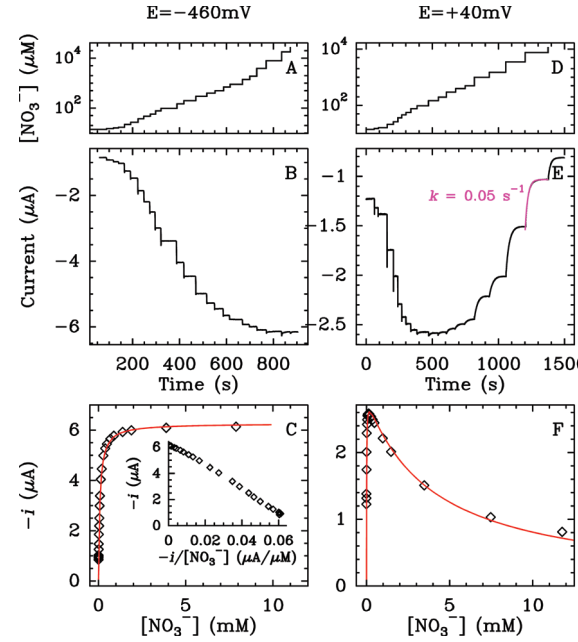

Figure 3. Dependence of the rate of nitrate reduction on nitrate concentration. The left- and right-hand sides correspond to a redox poise at −460 and +40 mV vs SHE, respectively. Conditions: pH 6; 25 °C; 5 krpm. Panels A and D show the evolution of nitrate concentration against time, when the concentration is stepwise increased by adding aliquots of a stock solution of potassium nitrate (note the logarithmic Y scale). Panels B and E show the resulting change in catalytic current. The data were corrected for film loss as described previously;[24] the raw data are shown on Supporting Information Figure S2. Panels C and F show the catalytic current reached at the end of each step as a function of nitrate concentration. The fit of the data in C to the Michaelis−Menten equation gives K_m = 85 μM. The inset shows a Eadie−Hofstee plot. The red line in panel F is the best fit to eq 2 with K_m = 10 μM and K_i = 4 mM. The purple trace on panel E corresponds to the very same conditions as those of the trace of the same color in Figure 2B.

decrease in current due to film desorption (plain and dashed lines in Figure 1B): the enzyme slowly activates under reducing conditions and inactivates under oxidizing conditions. This effect superimposes on the steady-state dependence of activity on E (Figure 1A) to produce the odd voltammogram in Figure 1B.

To disentangle the influence of the different experimental parameters on this phenomenon, we carried out chronoamperometric experiments in which either the electrode potential or the substrate concentration is stepwise varied, the resulting change in activity being monitored as a change in current.

Electrode Potential Steps. Figure 2 shows how the activity varies after stepping the electrode potential (E) when the nitrate concentration is 7.5 mM, pH 6. After each step, the activity relaxes exponentially toward a new steady-state value; it slowly increases (the current becomes more negative) after a step down and slowly decreases after a step up. Both the asymptotic value of the current and the rate of the relaxation depend on potential, but neither depends on the direction of the step or sample history (compare for example the two transients recorded at E = −60 mV plotted in red in Figure 2B). This shows that the active and inactive forms of the enzyme, A and I, respectively, interconvert with potential-dependent rate constants:

$$\mathrm{A} \underset{k_a}{\overset{k_i}{\rightleftharpoons}} \mathrm{I} \qquad (1)$$

The steady-state fraction of inactive enzyme depends on the equilibrium constant k_i/k_a. Importantly, the rates k of the exponential relaxations in Figure 2 are neither k_a nor k_i, but rather the sum of the two: $k = k_i + k_a$.[25] Supporting Information Figure S1 shows that k depends on E in a complex manner. In particular, it is the smallest at about 0 V vs SHE (depending on $[NO_3^-]$ and pH) and markedly increases at lower potential (this is clear even from the raw data in Figure 2). We also observed a slight increase of k at high potential under certain conditions of pH and nitrate concentration (see, e.g., the data at pH 5, 1 mM nitrate in Supporting Information Figure S1).

Interpreting the dependence of k on potential is not trivial because both k_i and k_a depend on potential. This is easily demonstrated as follows. We first rewrite $k = k_i(1 + k_a/k_i)$ and consider for example the step from +40 to −60 mV in Figure 2. We observe that k_a/k_i increases (the enzyme activates) and k decreases (albeit slightly); this implies that this potential step makes k_i decrease. Conversely, with use of the expression $k = k_a(1 + k_i/k_a)$ and from the observation in Figure 2 that upon stepping E from −60 to −160 mV, k_i/k_a decreases (the enzyme activates) and k increases, we conclude that k_a increases in this step.

Considering that reduction activates the enzyme (Figures 1 and 2), two hypotheses can explain the dependence of k_i on E. (i) The inactive form may be more oxidized than any species in the catalytic cycle and the inactivation is an oxidation, or (ii) the inactivation is a chemical step that is coupled to an oxidation, in which case the inactivation can proceed from catalytic intermediates having different redox states. Similarly, the fact that k_a depends on E suggests that the activation is either a reduction or a chemical step that is coupled to a reduction, in which case the inactive form must exist in several redox states.

Substrate Concentration Steps. Figure 3 shows the effects of stepwise increasing the nitrate concentration at two electrode potentials. When the electrode potential is low (E = −460 mV for the experiment in Figure 3, left), the activity instantly relaxes

toward a greater value after each addition of nitrate in the electrochemical cell (Figure 3B). The variation of steady-state activity merely follows Michaelis−Menten kinetics in the entire range of nitrate concentration (up to 30 mM), as demonstrated by the linearity of the Eadie−Hofstee plot in the inset of Figure 3C. (Note that in these experiments, the ionic strength of the solution is fixed by NaCl (100 mM) and the data in Figure 3C confirm that monovalent cations such as K^- (the counterion of nitrate) have no inhibitory effect on Nap.[26])

A very different and unexpected behavior is observed when the potential is less negative (e.g., $E = +40$ mV for the experiment in Figure 3, right). After a step in nitrate concentration, when the nitrate concentration is still small, the relaxation of activity is fast and cannot be measured (this is like the situation at low potential); in contrast, when the concentration is greater than about 100 μM, a *slow* relaxation toward a *lower* steady-state activity is observed (Figure 3E). These transients are monoexponential, with rates matching those deduced from potential-step experiments under the same conditions: for example the relaxation rate constants measured at $[NO_3^-] = 7.5$ mM and $E = +40$ mV are exactly equal (purple transients in Figures 2B and 3E). This demonstrates that the decreases in activity observed at high E and/or high nitrate concentration result from the same transformation.

The dependence of the steady-state activity on substrate concentration (Figure 3F) is well-described by assuming that an additional NO_3^- molecule binds to the enzyme−substrate complex to produce a fully inactive species characterized by a dissociation constant K_i:[25]

$$i = \frac{i_{max}}{1 + \frac{K_m}{[NO_3^-]} + \frac{[NO_3^-]}{K_i}} \quad (2)$$

The fit in Figure 3C returned $K_m = 85$ μM and $K_i > 1$ M at $E = -460$ mV, and in Figure 3F, $K_m = 8$ μM and $K_i = 4$ mM at $E = +40$ mV (pH 6, 25 °C in both cases). That the value of K_m depends on E was predicted by the model for the steady-state waveshape in refs 27 and 21. The value of K_i increases with pH (e.g., we determined $K_i = 50$ mM at pH 7, −20 mV). The fact that the rates of the relaxations after a step in potential or substrate concentration are the same (Figures 2 and 3) demonstrates that, in eq 2, $[NO_3^-]/K_i$ equates the ratio k_i/k_a (the pseudo-first-order rate constants defined in eq 1).

Substrate Inhibition in Solution Assays. Nitrate reductase activity is usually assayed by having the enzyme receiving electrons from a soluble redox mediator, whose rate of oxidation can be determined using UV−vis spectroscopy. We confirmed the above observation that the enzyme is inactivated by excess nitrate only at relatively high electrode potential by performing such solution assays with two redox dyes whose reduction potentials are very different. Figure 4 compares the time course of the oxidation of methyl viologen (MV; $E^0 = -440$ mV) and methylene blue (MB; $E^0 = -70$ mV). With the former, increasing nitrate concentration from 4 to 40 mM does not change the turnover rate (panel A). This is as expected, since these concentrations are much greater than the Michaelis constant (about 400 μM [17]). In contrast, panel B shows that the same stepwise increase in nitrate concentration *slows* methylene blue oxidation about 8-fold. The agreement with the results of PFV is even semiquantitative, since the 8-fold decrease in activity in Figure 4B is close to the factor of 5.5 that is predicted by eq 2 using the parameters determined from the experiments at +40 mV in Figure 3E.

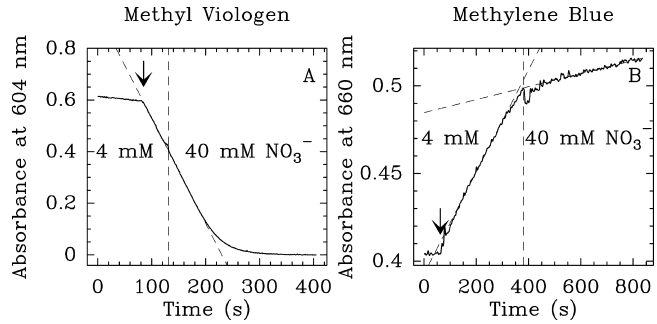

Figure 4. Substrate inhibition is solution assays. Conditions: pH 6; $T = 25$ °C; 4 mM and 40 mM nitrate respectively on the left- and right-hand sides of the vertical dashed line (the dilution resulting from adding an aliquot of concentrated solution of nitrate is negligible). In both panels, the arrow marks the addition of the enzyme in the cuvette. The redox mediator is initially reduced by adding sodium dithionite. On panel A, the redox dye is methyl viologen ($E^0 = -440$ mV, blue in its reduced form). The variation of the slope upon nitrate addition is smaller than 1%. On panel B, the mediator used is methylene blue ($E^0 = -70$ mV, blue in its oxidized form). Nitrate addition decreases the rate of MB oxidation by a factor of 8. The particular feature discussed in ref 22 is not seen in panel A because the pH and the initial concentration of reduced mV are both relatively low in this experiment.

Discussion

We have provided the first demonstration that high substrate concentrations inhibit periplasmic nitrate reductase. This is unprecedented in enzymes of the DMSO reductase family, but regarding periplasmic nitrate reductase, it is not surprising that this phenomenon had not been detected previously since it does not occur under the very reducing *initial* conditions which prevail when the enzyme activity is assayed with methyl viologen, the usual electron donor in solution assays. However, NapAB receives electrons from the quinol pool in the membrane, via a *c*-type cytochrome, whose hemes have reduction potentials in the range from −250 to −50 mV.[28] It is therefore likely that the extreme driving force provided by reduced MV is never reached in vivo and that the physiologically most important conditions are those of moderate driving force, where substrate inhibition actually occurs.

Considering our observations on the effect of nitrate concentration, we conclude that the inhibition should be insignificant at low nitrate concentrations (close to K_m), but it may be important to realize that NapAB being periplasmic, it is exposed to whichever nitrate concentration is present in the natural habitat or used in the culture medium. The latter is sometimes supplemented with very high concentrations of substrate (e.g., 50 mM in ref 29).

Whether the inhibition process is indicative of some useful (regulatory) process is unknown, but the observation that high concentrations of nitrate and mildly reducing conditions favor the formation of inactive species has important implications regarding the design and interpretation of biophysical experiments aimed at isolating catalytic intermediates of Nap. For example, Moura et al. identified by EPR two distinct Mo(V) species called "turnover"[8,30] and "nitrate"[30] after reoxidation of reduced *Desulfovibrio desulfuricans* (*D. desulfuricans*) Nap with 100 mM nitrate (pH 7.6). The "high-*g* split nitrate" signal of *P. pantotrophus* Nap, which is said to be catalytically relevant in ref 12, is also obtained with 100 mM nitrate (pH 7.2).[31] This

enzyme was reacted with 10 mM nitrate at pH 7.2 in the freeze-quench experiment reported in ref 32. In crystallography experiments, the *D. desulfuricans* Nap "nitrate soak" diffraction data set was obtained with a sample that was redox cycled, crystallized at pH 6, and then soaked with 10 mM nitrate.[8]

In our experiments, substrate inhibition is very pronounced at pH 6 or below, but it can also be very clearly detected under more alkaline conditions. Supporting Information Figure S3 compares the results of experiments carried out at pH 6 and 7; the deviation from Michaelis−Menten kinetics is still very clear at pH 7, where about 40% of inactive enzyme is formed at $E = -20$ mV, 30 mM nitrate. Considering that the species detected in EPR are always substoichiometric, the question arises as to whether they correspond to catalytic intermediates.

Although there is no proof so far that any isolated species correspond to the inactive form we have identified, we note that it has always been presumed that catalytically competent species would accumulate upon incubation of the enzyme with highly concentrated nitrate; our results clearly suggest otherwise.

We have observed that, all things being equal, stepping either the electrode potential or the nitrate concentration leads to a relaxation toward a new steady state at the same rate (compare for example the transients plotted in purple in Figures 2 and 3). This implies that the two types of transients result from the same equilibration process, that is the interconversion between active and inactive forms of the enzyme (as depicted in eq 1). That these relaxations are much slower than turnover implies that the catalytic cycle remains in a steady state during the transients. Canters and co-workers recently showed that the unrelated enzyme copper-containing nitrite reductase also exhibits substrate inactivation and reductive activation, but the situation is entirely different: in this enzyme, a slow reductive activation (Figure 3 in ref 33) reveals the reversible formation of a dead-end species, but, in contrast with NapAB, substrate inhibition is instantaneous (Figure 2 in ref 34) and results from a change of route in the mechanism, electron transfer to the active site occurring either before or after substrate binding.

We consider as most likely that the formation of the inactive species in NapAB relates to a transformation that occurs at, or in, the vicinity of the molybdenum cofactor, because mutating residues that are close to the active site significantly affect the inactivation process. Indeed, we could not detect any hysteresis or substrate inhibition in the voltammetry of enzymes whose active site pocket has been modified by site-directed mutagenesis. As an example, Figure 1C shows a voltammogram recorded with the R392A mutant at very high substrate concentration (R392 is in the vicinity of the active site, with one of the guanidinium N_η at 9.2 Å from the Mo). No hysteresis could be detected either with the Q384N and M153A variants (the side chain of Q384 is hydrogen bonded to the Mo; M153 is adjacent to C152, which directly ligates the Mo). [We note that these mutations increase the Michaelis constant at least 10-fold, which may result in a commensurate (or even greater) increase in K_i.] Regarding the WT enzyme, the fact that the extent of inactivation depends on substrate concentration and pH, unlike the reduction potentials of the electron-transfer relays in the enzyme,[21] also supports the view that the activation process is related to molybdenum chemistry.

By analyzing the potential steps experiments (in Figure 2 and Supporting Information Figure S1), we concluded that the enzyme reductively activates and that the rate of formation of the active species (k_a in eq 1) increases at low potential; this implies that the activation is either a pure reduction or a chemical step that is coupled to a reduction. We favor the latter

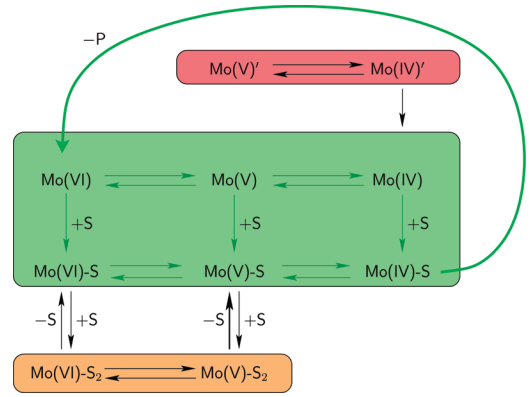

Figure 5. Connection between active and inactive states of NapAB. The species are plotted from Mo(VI) to Mo(IV) (left to right) as in our previous reports.[18,21] "±S" or "P" depicts the binding and release of substrate and product. The green box contains the species that are part of the catalytic cycle according to ref 21. The dead-end inactive form in the upper red box corresponds to the Mo(V) high-*g* species whose activation is slow, irreversible, and pH and nitrate concentration independent (as described previously[13]). The orange box frames the inactive forms studied here, whose formation is reversible and very dependent on potential, pH, and nitrate concentration.

hypothesis, because the experiment in Figure 3 (right) shows that activation consists of the release of a nitrate molecule (with dissociation constant K_i). Hence we conclude that the inactive form of the enzyme exists in several redox states and that the nitrate release step that activates the enzyme is coupled to the reduction of an oxidized inactive form. Since the formation of an inactive form upon *competitive* binding of a substrate molecule would not lead to inhibition at high nitrate concentration,[25] we concluded that the mechanism of substrate inhibition is uncompetitive (eq 2). The nitrate molecule that inhibits the enzyme must bind to catalytic intermediates in which the substrate is already bound, since the inhibition constant is much greater than the Michaelis constant. On the basis of the available structural data, it is difficult to speculate on the mode of nitrate binding. The inhibition constant increases at low E and high pH; the latter observation suggests that the nitrate binding step that inhibits the enzyme depends upon a protonation step.

Figure 5 shows the mechanism inferred from our data and refs 13 and 21.

The green box frames the *active* species that are potentially involved in the catalytic cycle. We have shown previously that this kinetic scheme can explain the shape of the steady-state voltammograms recorded at low concentration of nitrate, such as that in Figure 1A.[21,27] According to this model, catalysis can follow distinct routes, as, e.g., substrate binding either precedes or follows the reduction from Mo(V) to Mo(IV), and the relative rates of the two reactions determine which track is used, the Mo(V) state acting as a railway switch. The steady-state activity decreases at low electrode potential because turnover is slower when substrate binding follows reduction of Mo(V) to Mo(IV). We have previously emphasized the correlation between the position of the low potential feature of the steady-state voltammogram and the reduction potential of the Mo(V) species that exhibits the high-g signature.[21,27] However, because we now know that the Mo(V) signature actually corresponds to an inactive species,[13] this correlation appears to be fortuitous.

The inactive species detected in this work are in the lower, orange box in Figure 5. Their formation at high nitrate concentration and under mildly reducing conditions decreases the amount of active enzyme and causes the hysteresis that is seen only at high nitrate concentration (Figure 1B). It is

important to realize that this phenomenon is completely independent from the attenuation of steady-state activity at low electrode potential and all nitrate concentrations (observed, e.g., in Figure 1A). According to Figure 5, these inactive species are formed reversibly upon binding of a second nitrate molecule to either Mo(V) or Mo(VI), but not Mo(IV); this is consistent with the observation that substrate inhibition is not observed under very reducing reductions.

The red box frames the species whose activation is reported in ref 13. The dead-end Mo(V) species marked with a prime sign in this box has the spectral signature called "Mo(V) high *g*". Its activation is slow (<0.01 s^{-1} with NapAB), irreversible, pH and nitrate concentration independent and therefore entirely distinct from the reversible, reductive activation we described in this paper.

Conclusion

After decades of kinetic and spectroscopic studies of nitrate reductase, the catalytic mechanism is still very obscure: crystallographers recently challenged the accepted mechanism when they proposed that the Mo in the oxidized ("as-prepared") enzyme from *D. desulfuricans* is coordinated by the four thiolates of two pterins, a cysteine and a *sulfur* ligand, rather than the expected oxo.[8] Subsequent density functional theory studies aimed at evaluating the proposed mechanisms still favored nitrate binding to the Mo (rather than to the putative sulfur ligand); it is now proposed that, during catalysis, the Mo is actually coordinated by two pterins, a *persulfurated* cysteine which binds by just the terminal sulfur atom, and an oxygenated species.[10,11] Insights should have been provided by spectroscopic studies, but the main obstacle has been the inability to generate trustworthy catalytic intermediates in which a substrate moiety is bound to the Mo: various Mo(V) EPR signals have been detected, with no proof that any of them actually corresponds to a catalytic species. The activation and inactivation processes evidenced in this paper have revealed the existence of several forms of the enzyme which stand apart from the reaction pathway; since they accumulate under certain conditions of turnover (neutral or acidic pH, high nitrate concentration, mildly reducing conditions), they may easily be mistaken for catalytic intermediates. It is now likely that single turnover experiments, using stoichiometric rather than saturating concentrations of substrate, will be more useful for trapping catalytic intermediates of nitrate reduction. We hope that the results herein will help spectroscopists and crystallographers appraise former data and optimize experimental conditions in further studies.

Methods

The purification of the enzyme was described in refs 3 and 17. The catalytic properties of the mutants compare to the WT as follows:[17] WT, $v_{max} = 13\ \mu M\ min^{-1}\ mg^{-1}$ and $K_m = 0.4$ mM; R392A, $v_{max} = 12\ \mu M\ min^{-1}\ mg^{-1}$ and $K_m = 65$ mM; M153A, $v_{max} = 13\ \mu M\ min^{-1}\ mg^{-1}$ and $K_m = 3$ mM; Q384N, $v_{max} = 9\ \mu M\ min^{-1}\ mg^{-1}$ and $K_m = 1.1$ mM (this is determined in the presence of 2 mM reduced MV, in 100 mM Tris/HCl buffer at pH 8, 30 °C [17]).

The electrochemical equipment was described in ref 35. The enzyme films were prepared using neomycin as coadsorbate and a pyrolytic graphite edge rotating disk electrode (4 mm^2 surface), and then activated by electrochemically reducing the sample as described previously.[13] Using neomycin greatly increases the film stability. However, we have observed that, under certain conditions, neomycin on graphite gives peaks that look like noncatalytic signals; control experiments with no protein were used to discard these artifactual signals. The buffer consisted of a mixture of 2-(*N*-morpholino)ethanesulfonic acid (MES), 2-[*N*-cyclohexylamino]-ethenesulfonic acid (CHES), *N*-tris-[hydroxymethyl]methyl-3-aminopropanesulfonic acid (TAPS), *N*-(2-hydroxyethyl)-piperazine-*N*′-[2-ethanesulfonic acid] (HEPES), and sodium acetate (5 mM each) and 0.1 M NaCl, titrated to the desired pH using concentrated NaOH or HCl. Nitrate was added from stock solutions of potassium nitrate in water (1 mM or 2 M, depending on target concentration). All experiments were carried out in a glovebox, under an atmosphere of N_2.

Spectrophotometric assays were carried out using a homemade water-jacketed glass open cell (working volume, 0.5−1 mL) stirred with a rotating magnet and located in a glovebox, under an atmosphere of N_2. The absorbance was measured using a microprobe (Varian, Single arm, 10 mm path length, 3.05 mm diameter, 140 mm length) connected with an optic fiber (Varian, 3 m length) to a UV/visible spectrophotometer (Varian Cary 50). The absorbance was sampled at 10 Hz and averaged over 10 data points. Before adding the enzyme, methyl viologen or methylene blue was reduced by stepwise adding aliquots of a fresh solution of sodium dithionite. The extent of reduction was monitored spectroscopically to ensure that the reaction was complete and that no excess dithionite was left in the reaction buffer. The experimental conditions for the experiments in Figure 4 were as follows: with methyl viologen ($E^0 = -440$ mV) in panel A, $\varepsilon^{red}_{604} = 13600\ M^{-1}\ cm^{-1}$, total MV concentration of 5 mM, initial concentration of reduced MV of 45 μM, and final concentration of enzyme of 2 nM; with methylene blue ($E^0 = -70$ mV) in panel B, $\varepsilon^{ox}_{660} = 37900\ M^{-1}\ cm^{-1}$, total MB concentration of 25 μM, initial concentration of reduced MB of 18 μM, and final concentration of enzyme of 8 nM. In both cases the following conditions applied: pH 6, $T = 25$ °C, and $[NO_3^-] = 4$ mM and then 40 mM.

The data were analyzed with an in-house program called SOAS,[36] which is available via the Internet at http://bip.cnrs-mrs.fr/bip06.

Acknowledgment. We thank B. Burlat, B. Guigliarelli, and A. Magalon for fruitfull discussions. Our work is funded by the CNRS, CEA, ANR, Aix-Marseille Université, and the City of Marseilles.

Supporting Information Available: Figures S1−S3, showing the potential dependence of the relaxation rate constants, as-recorded and after-correction chronoamperograms, and substrate inhibition at pHs 6 and 7. This information is available free of charge via the Internet at http://pubs.acs.org.

References and Notes

(1) Barney, B. M.; Lukoyanov, D.; Igarashi, R. Y.; Laryukhin, M.; Yang, T.-C. C.; Dean, D. R.; Hoffman, B. M.; Seefeldt, L. C. *Biochemistry* **2009**, *48*, 9094–9102.
(2) Hoffman, B. M.; Dean, D. R.; Seefeldt, L. C. *Acc. Chem. Res.* **2009**, *42*, 609–619.
(3) Arnoux, P.; Sabaty, M.; Alric, J.; Frangioni, B.; Guigliarelli, B.; Adriano, J. M.; Pignol, D. *Nat. Struct. Mol. Biol.* **2003**, *10*, 928–934.
(4) Schwarz, G.; Mendel, R. R.; Ribbe, M. W. *Nature* **2009**, *460*, 839–847.
(5) Moura, J. J.; Brondino, C. D.; Trincao, J.; Romao, M. J. *J. Biol. Inorg. Chem.* **2004**, *9*, 791–799.
(6) Hille, R. *Trends Biochem. Sci.* **2002**, *27*, 360–367.
(7) Hille, R. *Chem. Rev.* **1996**, *96*, 2757–2816.
(8) Najmudin, S.; González, P. J.; Trincão, J.; Coelho, C.; Mukhopadhyay, A.; Cerqueira, N. M.; Romão, C. C.; Moura, I.; Moura, J. J.; Brondino, C. D.; Romão, M. J. *J. Biol. Inorg. Chem.* **2008**, *13*, 737–753.
(9) Hofmann, M. *J. Biol. Inorg. Chem.* **2007**, *12*, 989–1001.
(10) Cerqueira, N. M.; Gonzalez, P. J.; Brondino, C. D.; Romão, M. J.; Romão, C. C.; Moura, I.; Moura, J. J. *J. Comput. Chem.* **2009**, *30*, 2466–2484.

(11) Hofmann, M. *J. Biol. Inorg. Chem.* **2009**, *14*, 1023–1035.

(12) Jepson, B. J. N.; Mohan, S.; Clarke, T. A.; Gates, A. J.; Cole, J. A.; Butler, C. S.; Butt, J. N.; Hemmings, A. M.; Richardson, D. J. *J. Biol. Chem.* **2007**, *282*, 6425–6437.

(13) Fourmond, V.; Burlat, B.; Dementin, S.; Arnoux, P.; Sabaty, M.; Boiry, S.; Guigliarelli, B.; Bertrand, P.; Pignol, D.; Léger, C. *J. Phys. Chem. B* **2008**, *112*, 15478–15486.

(14) Bray, R.; Adams, B.; Smith, A.; Bennett, B.; Bailey, S. *Biochemistry* **2000**, *39*, 11258–11269.

(15) Léger, C.; Bertrand, P. *Chem. Rev.* **2008**, *108*, 2379–2438.

(16) Gates, A. J.; Richardson, D. J.; Butt, J. N. *Biochem. J.* **2008**, *409*, 159–168.

(17) Dementin, S.; Arnoux, P.; Frangioni, B.; Grosse, S.; Léger, C.; Burlat, B.; Guigliarelli, B.; Sabaty, M.; Pignol, D. *Biochemistry* **2007**, *46*, 9713–9721.

(18) Elliott, S. J.; Léger, C.; Pershad, H. R.; Hirst, J.; Heffron, K.; Blasco, F.; Rothery, R.; Weiner, J.; Armstrong, F. A. *Biochim. Biophys. Acta* **2002**, *1555*, 54–59.

(19) Rapson, T. D.; Kappler, U.; Bernhardt, P. V. *Biochim. Biophys. Acta* **2008**, *1777*, 1319–1325.

(20) Elliott, S. J.; Hoke, K. R.; Heffron, K.; Palak, M.; Rothery, R. A.; Weiner, J. H.; Armstrong, F. A. *Biochemistry* **2004**, *43*, 799–807.

(21) Bertrand, P.; Frangioni, B.; Dementin, S.; Sabaty, M.; Arnoux, P.; Guigliarelli, B.; Pignol, D.; Léger, C. *J. Phys. Chem. B* **2007**, *111*, 10300–10311.

(22) Fourmond, V.; Burlat, B.; Dementin, S.; Sabaty, M.; Arnoux, P.; Étienne, E.; Guigliarelli, B.; Bertrand, P.; Pignol, D.; Léger, C., published online Feb 10, http://dx.doi.org/10.1021/bi902140e.

(23) Jones, A. K.; Camba, R.; Reid, G. A.; Chapman, S. K.; Armstrong, F. A. *J. Am. Chem. Soc.* **2000**, *122*, 6494–6495.

(24) Fourmond, V.; Lautier, T.; Baffert, C.; Leroux, F.; Liebgott, P.-P.; Dementin, S.; Rousset, M.; Arnoux, P.; Pignol, D.; Meynial-Salles, I.; Soucaille, P.; Bertrand, P.; Léger, C. *Anal. Chem.* **2009**, *81*, 2962–2968.

(25) Cornish-Bowden, A. *Fundamental of Enzyme Kinetics*; Portland Press: London, U.K., 2004.

(26) Bursakov, S. A.; Carneiro, C.; Almendra, M. J.; Duarte, R. O.; Caldeira, J.; Moura, I.; Moura, J. J. *Biochem. Biophys. Res. Commun.* **1997**, *239*, 816–822.

(27) Frangioni, B.; Arnoux, P.; Sabaty, M.; Pignol, D.; Bertrand, P.; Guigliarelli, B.; Léger, C. *J. Am. Chem. Soc.* **2004**, *126*, 1328–1329.

(28) Roldan, M. D.; Sears, H. J.; Cheesman, M. R.; Ferguson, S. J.; Thomson, A. J.; Berks, B. C.; Richardson, D. J. *J. Biol. Chem.* **1998**, *273*, 28785–28790.

(29) Sabaty, M.; Schwintner, C.; Cahors, S.; Richaud, P.; Vermeglio, A. *J. Bacteriol.* **1999**, *181*, 6028–6032.

(30) Gonzalez, P. J.; Rivas, M. G.; Brondino, C. D.; Bursakov, S. A.; Moura, I.; Moura, J. J. G. *J. Biol. Inorg. Chem.* **2006**, *11*, 1432–1327.

(31) Butler, C.; Charnock, J.; Bennett, B.; Sears, H.; Reilly, A.; Ferguson, S.; Garner, C.; Lowe, D.; Thomson, A.; Berks, B.; Richardson, D. *Biochemistry* **1999**, *38*, 9000–9012.

(32) Butler, C. S.; Fairhurst, S. A.; Ferguson, S. J.; Thomson, A. J.; Berks, B. C.; Richardson, D. J.; Lowe, D. J. *Biochem. J.* **2002**, *363*, 817–823.

(33) Wijma, H. J.; Jeuken, L. J. C.; Verbeet, M. P.; Armstrong, F. A.; Canters, G. W. *J. Am. Chem. Soc.* **2007**, *129*, 8557–8565.

(34) Wijma, H. J.; Jeuken, L. J. C.; Verbeet, M. P.; Armstrong, F. A.; Canters, G. W. *J. Biol. Chem.* **2006**, *281*, 16340–16346.

(35) Liebgott, P.-P.; et al. *Nat, Chem. Biol.* **2010**, *6*, 63–70.

(36) Fourmond, V.; Hoke, K.; Heering, H. A.; Baffert, C.; Leroux, F.; Bertrand, P.; Léger, C. *Bioelectrochemistry* **2009**, *76*, 141–147.

(37) Xie, H.; Cao, Z. *Organometallics* **2010**, *29*, 436–441.

JP911443Y